

# New Global F-theory GUTs with $U(1)$ symmetries

Volker Braun<sup>1</sup>, Thomas W. Grimm<sup>2</sup> and Jan Keitel<sup>2</sup>

<sup>1</sup> Dublin Institute for Advanced Studies,  
10 Burlington Road, Dublin 4, Ireland

<sup>2</sup> Max-Planck-Institut für Physik,  
Föhringer Ring 6, 80805 Munich, Germany

## ABSTRACT

We construct global F-theory GUTs with  $SU(5) \times U(1)$  gauge group defined by specifying a fully resolved Calabi-Yau fourfold and consistent four-form G-flux. Its specific  $U(1)$  charged matter spectrum allows the desired Yukawa couplings, but forbids dangerous proton decay operators. The model we find: (1) does not follow from an underlying higgsed  $E_8$  gauge group (2) leaves the class of theories that can be analysed, even locally, with current split-spectral cover techniques. This allows to avoid various recently proposed no-go theorems for models with hypercharge flux required to break the GUT group. The appearance of additional fields is related geometrically to considering a more general class of sections and 4-1 splits. We show explicitly that the four-dimensional chiral matter index can still be computed using three-dimensional one-loop Chern-Simons terms.

# 1 Introduction and Summary

Over the past years, considerable effort has been spent on engineering phenomenologically viable  $SU(5)$ -GUTs in F-theory. This was initiated in local models with decoupled gravity in [1–3]. Since then, vast progress has been made both in providing a more detailed local construction as well as in finding global completions [4, 5]. Despite various successes, for example, the construction of fully resolved fourfolds with  $SU(5)$  and  $SO(10)$  gauge group singularities [6–10], fully consistent phenomenological models have yet to be found. This can, at least in a large class of GUT scenarios, be traced back to the fact that  $U(1)$  symmetries [11–16] are difficult to control in F-theory. This is naturally so because they do, unlike non-Abelian gauge factors, depend on the global properties of the Calabi-Yau manifold. Moreover, Abelian gauge factors can be crucial in order to prohibit proton decay in GUT models. That is, appropriate  $U(1)$ -charges can be used to allow only the desired couplings and forbid proton decay inducing couplings. However, the  $U(1)$  charges depend on the global Calabi-Yau geometry and are difficult to engineer.

In [17–19] a semi-local approach was used in order to construct models with  $SU(5) \times U(1)^k$  for  $k \leq 4$ . Since neither the  $U(1)$  gauge fields nor matter transforming as a singlet under  $SU(5)$  are localized on the GUT surface, these methods needed to be extended globally. In [14, 16], a certain class of global models based on a particular Ansatz for the section in the Weierstrass model was constructed. Following either one of these two approaches, the appearance of  $k$  extra  $U(1)$  gauge symmetries is attributed to the factorization of a degree five polynomial into  $k + 1$  factors. In the semi-local approach the defining equation of the spectral cover factorizes (that is, the cover splits) and in the global picture the Tate polynomial factors, enforcing the existence of additional sections of the fourfold. Accordingly, two different classes of models with  $SU(5) \times U(1)$  gauge

Model	Matter spectrum	
4–1 split	$\mathbf{5}_{-3}, \mathbf{5}_2, \mathbf{10}_{-1}, \mathbf{10}_4$	$\mathbf{1}_5$
3–2 split	$\mathbf{5}_{-4}, \mathbf{5}_1, \mathbf{5}_6, \mathbf{10}_{-3}, \mathbf{10}_2$	$\mathbf{1}_5, \mathbf{1}_{10}$

**Table 1.1:** Different  $SU(5) \times U(1)$  spectra originating from  $E_8$  branching rules.

group were found: the 4–1 split and the 3–2 split, where the numbers denote the order of the two irreducible factors. We note that the choices made in the Ansatz are reflected by the fact that only two out of three logically possible cases arise, namely a possible 5–0 split is absent. Also the matter spectra are rather restricted as listed in Table 1.1. Assuming the above field content, conditions for the existence of non-trivial hypercharge flux were analyzed [20]. For a single  $U(1)$  gauge group, anomaly cancellation after breaking  $SU(5)$  to the standard model gauge group imposes four linear equations on the flux quanta. Since the 4–1 split was found to have only four distinct matter curves, it was claimed that no consistent hypercharge flux can exist in these models.

However, both the split-spectral cover technique and the Ansatz for the section in [16–19] rely on the crucial assumption that the  $SU(5) \times U(1)$  gauge group originates from

a partially higgsed underlying  $E_8$  symmetry. To be precise, the GUTs in these analyses arise from the breaking

$$E_8 \longrightarrow SU(5)_{GUT} \times SU(5)_\perp \longrightarrow SU(5)_{GUT} \times U(1)^4 \quad (1.1)$$

and the respective branching of the adjoint representation of  $E_8$ . Using monodromies of the spectral cover [11, 21], some of the  $U(1)$  can then be identified, leading for example to  $SU(5) \times U(1)$ .

In this paper, we relax the assumption of an underlying higgsed  $E_8$  and show that more general global models arise naturally. To do so, we proceed as follows. First, Section 2 discusses a certain set of representations reminiscent of the 4–1 split containing  $\mathbf{10}_{-1}$  and  $\mathbf{5}_q$  satisfying

$$q \bmod 5 = 2 \quad (1.2)$$

just as in the models based on  $E_8$ . We describe how to match the representations with the MSSM field content in order to prohibit both dimension four proton decay and a tree-level  $\mu$ -term using a PQ-type symmetry and we show that non-trivial hypercharge fluxes are allowed. In Sections 3 and 4 we then explicitly construct the Calabi-Yau fourfold using methods from toric geometry and determine the spectrum. The appearance of additional matter is interpreted geometrically and attributed to more general types of sections wrapping entire fiber components instead of just single points. Last of all, we specify an explicit set of consistent four-form fluxes in Section 5. Using three-dimensional one-loop Chern-Simons terms, we compute the chiral indices of the four-dimensional matter representations and show that the spectrum is anomaly free.

## 2 More general GUT Models: Field Theory

Let us start with a brief field theoretic description of the model that we will construct in the remainder of this paper. The representation content of our four-dimensional theory is

$$\mathbf{10}_{-1}, \mathbf{5}_{-8}, \mathbf{5}_{-3}, \mathbf{5}_2, \mathbf{5}_7, \mathbf{1}_5, \mathbf{1}_{10}, \quad (2.1)$$

where the conjugate representations are understood to be included as well. Recalling that the necessary Yukawa couplings in order to reproduce the MSSM are

$$\mathbf{10}_M \mathbf{10}_M \mathbf{5}_H \quad \text{and} \quad \mathbf{10}_M \bar{\mathbf{5}}_M \bar{\mathbf{5}}_H, \quad (2.2)$$

we match the MSSM representations as

$$\bar{\mathbf{5}}_M \longleftrightarrow \bar{\mathbf{5}}_{-7} \quad \mathbf{5}_H \longleftrightarrow \mathbf{5}_2 \quad \bar{\mathbf{5}}_H \longleftrightarrow \bar{\mathbf{5}}_8 \quad \mathbf{10}_M \longleftrightarrow \mathbf{10}_{-1}. \quad (2.3)$$

Note that one could also swap the  $U(1)$ -charges assigned to  $\bar{\mathbf{5}}_M$  and  $\bar{\mathbf{5}}_H$ . With the above choice, both the dimension four proton decay operator

$$\mathbf{10}_M \mathbf{5}_M \mathbf{5}_M \quad (2.4)$$

as well as a tree-level  $\mu$ -term in the superpotential

$$\mu \mathbf{5}_H \bar{\mathbf{5}}_H \quad (2.5)$$

are forbidden by the  $U(1)$ -symmetry. The absence of the latter terms is equivalent to prohibiting operators such as

$$\mathbf{10}_M \mathbf{10}_M \mathbf{10}_M \bar{\mathbf{5}}_M, \quad (2.6)$$

which would induce dimension 5 operators after integrating out heavy modes. Let us remark that  $U(1)$ -symmetries with charge assignments such that

$$Q(\mathbf{5}_H) \neq -Q(\bar{\mathbf{5}}_H) \quad (2.7)$$

are called Peccei-Quinn (PQ) symmetries. The remaining representation  $\mathbf{5}_{-3}$  will carry exotic matter, while the  $SU(5)$ -singlets are candidates for right-handed neutrinos.

Having introduced the spectrum, we now turn to the conditions any anomaly-free spectrum must satisfy. Before turning on hypercharge flux to break up the above  $SU(5)$ -multiplets, these conditions are

$$\begin{aligned} 0 &= \chi(\mathbf{10}_{-1}) + \sum_q \chi(\mathbf{5}_q), \\ b_{(5)}^\alpha \Theta_{\alpha 5} &= -\frac{20}{3} \chi(\mathbf{10}_{-1}) + \frac{10}{3} \sum_q \chi(\mathbf{5}_q) q^3 + \frac{2}{3} \sum_p \chi(\mathbf{1}_p) p^3, \\ -a^\alpha \Theta_{\alpha 5} &= -\frac{10}{3} \chi(\mathbf{10}_{-1}) + \frac{5}{3} \sum_q \chi(\mathbf{5}_q) q + \frac{1}{3} \sum_p \chi(\mathbf{1}_p) p, \\ b^\alpha \Theta_{\alpha 5} &= 6\chi(\mathbf{10}_{-1}) + 2 \sum_q \chi(\mathbf{5}_q). \end{aligned} \quad (2.8)$$

They follow from demanding that the non-Abelian anomaly, the purely Abelian anomaly and two mixed anomalies are cancelled, respectively. The index  $q \in \{-8, -3, 2, 7\}$  ranges over the different charges of the  $\mathbf{5}$ -representations and  $p$  runs over the  $U(1)$ -charges of the  $SU(5)$ -singlets.  $a^\alpha$ ,  $b^\alpha$  and  $b_{(5)}^\alpha$  are coefficients of the Green-Schwarz terms and  $\Theta_{\alpha 5}$  is a Chern-Simons coefficient, all of which will be related to compactification data in Subsection 3.3.

After turning on hypercharge flux an additional set of conditions must be imposed. These can be understood as constraining all possible hypercharge fluxes. For a single  $U(1)$ , there are four constraints, namely

$$\begin{aligned} N_{10}^{-1} &= \sum_q N_5^q = 0, \\ -N_{10}^{-1} + \sum_q N_5^q q &= 0, \\ 3N_{10}^{-1} + \sum_q N_5^q q^2 &= 0, \end{aligned} \quad (2.9)$$

where  $N_b^a$  denotes the number of flux quanta along  $\mathbf{b}_a$ . Since we have five parameters and four linear constraints, the above equations admit a one parameter set of solutions:

$$\begin{aligned} N_{10}^{-1} &= 0, \\ N_5^{-8} &= \lambda, & N_5^{-3} &= -3\lambda, \\ N_5^2 &= 3\lambda, & N_5^7 &= -\lambda. \end{aligned} \tag{2.10}$$

We close this section by emphasizing that the former “no-go”-theorem forbidding hypercharge flux in models with 4–1 split is circumvented by the fact that there exist *five* distinct matter representations charged under  $SU(5)$ . To be precise, the anomaly constraints (2.9) and their generalized version for cases with several distinctly charged **10** representations [20] always eliminate precisely four flux parameters, as we see above. The “no-go”-theorem was solely based on a counting argument, since the 4-1 splits in models with an underlying  $E_8$  symmetry never have more than four distinct matter curves charged under  $SU(5)$  and therefore the only solution to the anomaly equations was to have no flux. However, we will show in the next section that there indeed exist models of a very similar type that can have more representations and therefore do admit non-trivial hypercharge flux. Furthermore, the existence of additional matter curves allows one to realize a PQ-symmetry in a model with 4–1 split, another feature that was formerly ruled out, since it requires the existence of at least three distinct **5** representations.

Nevertheless, we will not attempt to construct a phenomenologically viable model in this paper. In particular, we will not try to fix multiplicities to obtain three generations with the correct doublet-triplet splitting. However, the point that we do wish to make is that, in the context of F-theory compactifications, there arise naturally Abelian factors in the gauge group whose matter representations do not unify into a spontaneously broken  $E_8$ . Such theories can easily circumvent phenomenological stumbling blocks that have been found previously. A more complete study of the systematics of  $SU(5) \times U(1)$  models is underway [22].

### 3 Calabi-Yau Geometry and its Sections

In this section we introduce the fully resolved Calabi-Yau geometries relevant for the  $SU(5) \times U(1)$  GUT models with the spectrum given in Section 2. In Subsection 3.1 we summarize some basics about elliptic fibrations. We argue that the pattern of  $U(1)$  charges naturally allows to introduce ‘splits’ independent of the factorisation of defining equations or a spectral cover. The Calabi-Yau threefold and fourfold examples supporting our GUT spectrum are introduced in Subsection 3.2 and 3.3. We carefully discuss the sections of these elliptic fibrations.

### 3.1 Basics on Elliptic Fibrations with $SU(5) \times U(1)$

Before focusing on a specific example, let us quickly review the geometric features of elliptic fibrations as relevant for F-theory models with  $SU(5) \times U(1)$  gauge symmetry. Compactification of F-theory on an elliptically fibered threefold or fourfold yields a six- and four-dimensional effective theory respectively. In fact, one is interested in a singular Calabi-Yau manifold obtained by shrinking all irreducible fiber components not intersecting the zero section. These singularities give rise to non-Abelian gauge symmetries. However, arbitrary singularities are not allowed and it is probably necessary that there exists a resolution to a smooth Calabi-Yau. Therefore one can either consider smooth Calabi-Yau manifolds where one can always contract the fiber components not intersecting the zero section, or one can work with singular Calabi-Yau manifolds but then has to prove that a resolution exists.

By definition, an elliptic fibration is a surjective map  $\pi : X \rightarrow \mathcal{B}$  from the Calabi-Yau variety to a base  $\mathcal{B}$  whose generic fiber is  $T^2$  and such that there is a section. The fiber degenerates along a divisor in the base  $\mathcal{B}$  called the discriminant. The generic degenerate fibers have been classified by Kodaira and fall into an ADE-like pattern. For the purposes of this paper, we will be mostly interested in the  $I_n$  Kodaira fibers (the  $A_{n-1}$  series). Their dual graph (drawing a node for each  $\mathbb{P}^1$  irreducible component and a connecting line if they intersect) is the cycle graph with  $n$  nodes. Without monodromies the  $I_n$  Kodaira fiber yields a low-energy  $A_{n-1} = SU(n)$  gauge theory, which is what we will be interested in. More special fibers need not fall into the Kodaira classification starting at codimension-two in the base (codimension one along the discriminant). For starters, the codimension-two fibers may actually be higher-dimensional, a feature that we like to avoid in our F-theory models.

We can distinguish two kinds of sections, and both will feature prominently in this paper. The first and simpler case is that of a holomorphic section (or just section), meaning that there is a holomorphic embedding  $s : \mathcal{B} \hookrightarrow X$  of the base in the elliptic fibration such that the composition  $\pi \circ s = \text{id}_{\mathcal{B}}$  is the identity map on  $\mathcal{B}$ . The second and more complicated case is that of a rational section, that is, we require only a birational morphism  $s' : \mathcal{B} \dashrightarrow \mathcal{B}' \subset X$  such that  $\pi \circ s' = \text{id}_{\mathcal{B}}$ . This means that  $s' : \mathcal{B} \rightarrow \mathcal{B}'$  is generically one-to-one, but not defined over some points. The points where  $s'$  cannot be defined is where the divisor  $\mathcal{B}' \subset X$  wraps a whole fiber component. Clearly, a holomorphic section is a special case of a rational section. But we stress that rational sections are perfectly fine for F-theory compactifications, if somewhat overlooked in the physics literature. For physics applications, the rational sections give us important additional freedom: A holomorphic section must intersect any fiber in a single point, that is, it intersects a single irreducible fiber component with intersection number one. Rational sections, on the other hand, can wrap components of codimension-two fibers and therefore have more freedom in the intersection numbers. This translates into less constraints for the  $U(1)$  matter charges, as we will see in the following.

By definition, an elliptic fibration has at least one section. We pick one and call it the

zero section; physics does not depend on this choice. The set of all sections then forms an Abelian group under fiber-wise addition. That is, identify the torus  $T^2 = \mathbb{C}/(\mathbb{Z} \oplus \tau\mathbb{Z})$  such that the zero section passes through  $0 \in \mathbb{C}$ . Any pair of section then passes through two points, which can be added in  $\mathbb{C}/(\mathbb{Z} \oplus \tau\mathbb{Z})$  to obtain another section. The sections together with this group law are called the *Mordell-Weil* group  $MW(X)$ . Its rank is the number of independent  $U(1)$  gauge factors. We will be mostly interested in the rank-one case in the remainder of this paper, where there is an (up to sign) unique section that generates  $MW(X) \simeq \mathbb{Z}$ .

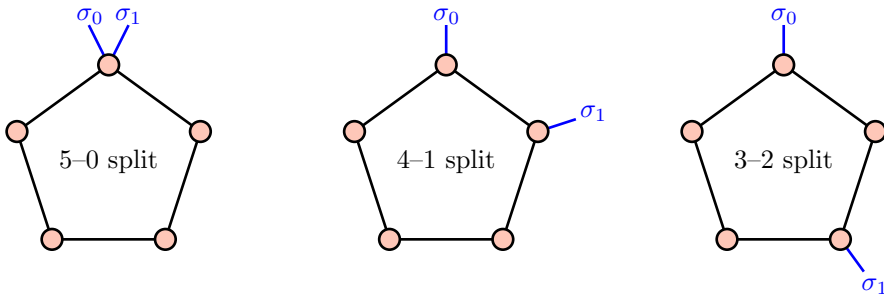


**Figure 1:** The three different relative orientations of the  $I_5$  discriminant and two sections  $\sigma_0, \sigma_1$ .

To obtain an  $SU(5) \times U(1)$  low-energy gauge theory, we thus need an  $I_5$  discriminant locus without monodromy together with two sections (the zero section and the Mordell-Weil generator). Up to relabelling, there are three different ways for the  $I_5$  and two sections to intersect which are depicted in Figure 1.

These three possibilities translate into different patterns of  $U(1)$  charges for matter fields. Note that  $U(1)$  charges can be normalized arbitrarily, for example it is sometimes claimed that the up quark has electric charge  $\frac{2}{3}$ . We will be using the sane normalization where the minimal charge is one. With this nomenclature, the three possibilities are

5–0 split: The  $SU(5)$  singlets have minimal  $U(1)$  charge one.

4–1 split: The  $SU(5)$  singlets have  $U(1)$  charges in  $5\mathbb{Z}$ . The  $\mathbf{5}$  of  $SU(5)$  (fundamental representation) have  $U(1)$  charge  $2, 3 \pmod{5}$ . The  $\mathbf{10}$  (antisymmetric representation) have  $U(1)$  charges  $1, 4 \pmod{5}$ .

3–2 split: The  $SU(5)$  singlets have  $U(1)$  charges in  $5\mathbb{Z}$ . The fundamentals have  $U(1)$  charges  $1, 4 \pmod{5}$ . The antisymmetrics have  $U(1)$  charges  $2, 3 \pmod{5}$ .

In special examples the two sections can be obtained by imposing that some polynomial related to the Calabi-Yau hypersurface equation factorizes. Note, however, that the 5–0 split has obviously nothing to do with a factorization of a degree-5 polynomial into a degree-5 and a degree-0 polynomial and does therefore not appear in the constructions of [16–19].

Point $n_z \in \nabla \cap N$	Coordinate $z$	Divisor $V(z)$
-1 -1 -1 -1	$h_0$	$\hat{H}_0$
0 0 0 1	$h_1$	$\hat{H}_1$
-2 -1 1 0	$d_0$	$\hat{D}_0$
-1 0 1 0	$d_1$	$\hat{D}_1$
0 0 1 0	$d_2$	$\hat{D}_2$
0 -1 1 0	$d_3$	$\hat{D}_3$
-1 -1 1 0	$d_4$	$\hat{D}_4$
-1 0 0 0	$f_0$	$\hat{F}_0$
0 1 0 0	$f_1$	$\hat{F}_1$
1 0 0 0	$f_2$	$\hat{F}_2$
-1 -1 0 0	$f_3$	$\hat{F}_3$

**Table 3.1:** The toric data for the smooth Calabi-Yau threefold  $X$ . Together with the origin, these are the only integral points in the lattice polytope  $\nabla$  and we will be using the notation on the right for the corresponding toric divisors. The Hodge numbers are  $h^{11}(X) = 7$  and  $h^{21}(X) = 63$ . Together with the fact that there is a  $I_5$  discriminant component, the Shioda-Tate-Wazir formula [23] tells us that  $\text{rank } MW(X) = 1$ . The fan is given in (A.1).

## 3.2 Calabi-Yau Threefold and its Sections

In this paper, we will be investigating F-theory compactifications on elliptically fibered Calabi-Yau fourfolds. In particular, we will be interested in the  $U(1)$  charges of matter fields, which are determined by codimension-two fibers. Hence this question is about the geometry of a three-dimensional variety and nothing in the analysis changes in an essential manner when we go from three- to fourfolds with the same fiber structure. Therefore, we will first discuss some crucial aspects in the context of Calabi-Yau threefolds in this section. For simplicity, we will be looking at the simplest possible base  $\mathbb{P}^2$ , though it would be very easy to apply our methods to more complicated toric bases or to complete intersections where the additional equations are constant along the fiber direction.

To be completely explicit, we will be considering the Calabi-Yau hypersurface [24] in the ambient toric variety specified by Table 3.1. The hypersurface in the 4-d toric variety is cut out by the equation

$$p = \sum_{m \in \Delta \cap M} \alpha_m h_0^{n_{h_0} \cdot m + 1} h_1^{n_{h_1} \cdot m + 1} d_0^{n_{d_0} \cdot m + 1} \dots f_3^{n_{f_3} \cdot m + 1} = 0 \quad (3.1)$$

where  $\Delta$  is the dual (polar) polytope to  $\nabla$ , and  $M$  is the dual lattice to  $N$ . The elliptic fibration is a toric morphism, that is, induced by a map of the fan  $\Sigma$  of the toric ambient space, given explicitly in Eq. (A.1), to the fan of  $\mathbb{P}^2$  by projecting on the last two coordinates of  $N \simeq \mathbb{Z}^4$ . In terms of homogeneous coordinates, the projection map  $\pi : X \rightarrow \mathbb{P}^2$



is given by

$$\pi : [h_0 : h_1 : d_0 : \dots : d_4 : f_0 : \dots : f_3] \mapsto [h_0 : h_1 : d_0 d_1 d_2 d_3 d_4] \quad (3.2)$$

We see that the homogeneous coordinates  $f_0, \dots, f_3$  corresponding to the rays in the kernel of the projection parametrize the fiber in the ambient space. The  $I_5$  discriminant component is the curve  $[z_0 : z_1 : 0] \in \mathbb{P}^2$  and the 5 divisors  $\hat{D}_0, \dots, \hat{D}_4$  map to it. In a generic fiber of the discriminant (codimension-one over the base), the Calabi-Yau hypersurface cuts out a  $\mathbb{P}^1$  in each of the 5 components, yielding the  $I_5$  Kodaira fiber.

The simplest way to define a section is to pick a toric divisor on the generic fiber, that is, set one of the  $f_i$  to zero. Together with the hypersurface equation, this cuts out a certain number of points in each fiber. The number of points can be computed using intersection theory, or naively by plugging in  $f_i = 0$  into the hypersurface equation. Homogeneous coordinates whose points are not in the star of the cone  $\langle n_{f_0} \rangle$  cannot vanish simultaneously with  $f_0$  and can be scaled to one.<sup>2</sup> Setting  $f_0 = 0, f_2 = d_i = 1, i > 0$  the hypersurface equation (3.1) takes the form

$$p : \alpha_0 f_1 + (\alpha_1 h_0^2 + \alpha_2 h_0 h_1 + \alpha_3 h_1^2 + \alpha_4 h_0 d_0 + \alpha_5 h_1 d_0 + \alpha_6 d_0^2) f_3 = 0. \quad (3.3)$$

This equation can be solved trivially for the homogeneous fiber coordinates  $[f_1 : f_3]$  along the  $\hat{F}_0$  divisor. In fact,  $f_1 \neq 0 = f_3$  is forbidden if all coefficients  $\alpha_m$  are sufficiently generic, so we may scale  $f_3 = 1$  as well. Thus, the section is

$$\begin{aligned} \sigma_0 : [h_0 : h_1 : d_0] &\mapsto [h_0 : h_1 : d_0 : 1 : 1 : 1 : 1 : 0 : f_1(h_0, h_1, f_0) : 1 : 1], \\ f_1(h_0, h_1, f_0) &= -\frac{1}{\alpha_0} (\alpha_1 h_0^2 + \alpha_2 h_0 h_1 + \alpha_3 h_1^2 + \alpha_4 h_0 d_0 + \alpha_5 h_1 d_0 + \alpha_6 d_0^2). \end{aligned} \quad (3.4)$$

We see that  $\sigma_0 = \{p = f_0 = 0\}$  is not only a section, which could have been learned from intersection theory alone, but also that it is a holomorphic section.

It remains to find a second section, namely the generator of the Mordell-Weil group. This is made more interesting by the fact that none of the remaining toric fiber divisors  $\hat{F}_1, \hat{F}_2, \hat{F}_3$  defines a section for us. In fact,  $\hat{F}_1$  and  $\hat{F}_3$  define two-sections and  $\hat{F}_2$  a three-section. Hence we will approach this section differently, and, instead of explicitly finding its equation, we will determine its homology class. A first guess, which is wrong but instructive, is to take  $[\hat{F}_1 - \hat{F}_0]$ . It is a two-section minus a section and therefore, numerically, a section. In more elaborate terms,<sup>3</sup> the generic fiber has the homology class  $\hat{H}_0 \cap \hat{H}_1 = \pi^{-1}([0 : 0 : 1])$ . By a simple intersection computation, its intersection with the tentative section is therefore

$$[\hat{F}_1 - \hat{F}_0] \cap \hat{H}_0 \cap \hat{H}_1 = 1. \quad (3.5)$$

<sup>2</sup>These coordinates lie in the Stanley-Reisner ideal when multiplied with  $f_0$

<sup>3</sup>Note that the divisors  $\hat{H}_0 = \pi^{-1}([0 : * : *])$  and  $\hat{H}_1 = \pi^{-1}([* : 0 : *])$  are elliptic fibrations over the coordinate  $\mathbb{P}^1$  in the base that intersect the discriminant transversely.

However, other intersection numbers show that the class  $[\hat{F}_1 - \hat{F}_0]$  does not contain a section. By intersecting the fibral<sup>4</sup> divisors with  $\hat{H}_0, \hat{H}_1$  we obtain the irreducible component curves  $C_i \simeq \mathbb{P}^1$  of the  $I_5$  Kodaira fibers as

$$C_i = \hat{D}_i \cap \hat{H}_0 = \hat{D}_1 \cap \hat{H}_1. \quad (3.6)$$

Computing the intersection numbers with the tentative section, we obtain

$$[\hat{F}_1 - \hat{F}_0] \cap C_i = [\hat{F}_1 - \hat{F}_0] \cap \hat{D}_i \cap \hat{H}_0 = \begin{cases} -1 & i = 0, \\ 1 & i = 1, 2, \\ 0 & i = 3, 4. \end{cases} \quad (3.7)$$

The fact that the intersection number is negative means that the  $I_5$  component curve  $C_0$  is contained  $[\hat{F}_1 - \hat{F}_0]$  as we slide it along over the discriminant. That is, the whole fibral divisor  $\hat{D}_0$  is contained in  $[\hat{F}_1 - \hat{F}_0]$ . But since a rational section may only contain components of codimension-two fibers and not complete fibral divisors (which are codimension-one over the base),  $[\hat{F}_1 - \hat{F}_0]$  is not a rational section after all. However, it is clear that this can be fixed by subtracting the fibral divisor  $\hat{D}_0$ .

Therefore our new best guess for the class of the section generating the Mordell-Weil group is  $[\hat{F}_1 - \hat{F}_0 - \hat{D}_0]$ . Computing intersection numbers, one finds that it still does not work and one needs to subtract further vertical divisors. After repeating the same steps several times, the end result is the homology class

$$[\sigma_1] = [\hat{F}_1 - \hat{F}_0 - \hat{D}_0 - \hat{D}_3 - \hat{D}_4 + \hat{H}_0]. \quad (3.8)$$

Showing that this homology class actually contains a section is more involved and will be presented in Subsection A.2. This is the section generating the Mordell-Weil group and, as we will see in the following, it is only a rational section. Computing the intersection number  $\sigma_1 \cap \hat{D}_1 \cap \hat{H}_0$  and noticing that  $\sigma_0$  intersects  $\hat{D}_0$  only from Eq. (3.4), we note that this elliptic fibration is of the 4-1 split type. Finally, we note from the sheaf cohomology computation that the section  $\sigma_1$  exists only on the Calabi-Yau hypersurface and does not extend to a section on the whole ambient toric variety. This is why its construction has been so tedious.

### 3.3 Calabi-Yau Fourfold and its Sections

As we have mentioned previously, the matter content induced by a particular Calabi-Yau manifold depends on the codimension-two singularities of the variety and one can extend the base from  $\mathbb{P}^2$  to  $\mathbb{P}^3$  without changing the types of matter representations that can occur. Extending the toric data in Table 3.1 to a fourfold is therefore very simple: We embed the points  $n_z$  into  $N' \simeq \mathbb{Z}^5$  via

$$n_z \mapsto \begin{cases} (n_z, 0) & \text{for } z \neq h_0 \\ (n_z, -1) & \text{for } z = h_0 \end{cases} \quad (3.9)$$

---

<sup>4</sup>The *fibral* divisors  $\hat{D}_i$  are the divisors swept out by irreducible component of the  $I_5$  Kodaira fiber as we move the curves along over the discriminant.

and add an additional point  $n_{h_2} = (0, 0, 0, 0, 1)$  whose divisor we denote by  $\hat{H}_2$ . By abuse of notation, we will use the same letters for divisors and homogeneous coordinates. Since we will never be talking about the Calabi-Yau fourfold and the threefold at the same time, their meaning should be clear from context.

Of the six triangulations that induce inequivalent intersection numbers on the Calabi-Yau hypersurface in the ambient toric fivefold, we choose the one given by (A.2). We remark that for this choice the zero section corresponding to  $f_0 = 0$  is not holomorphic anymore. However, this is no problem for F-theory applications. By the exact same reasoning as before, we find that there is (up to sign) a single Mordell-Weil generator. Its homology class is almost identical to the one in Eq. (3.8), namely

$$[\sigma_1] = [\hat{F}_1 - \hat{F}_0 - \hat{D}_0 - \hat{D}_3 - \hat{D}_4 + 2\hat{H}_0] . \quad (3.10)$$

To make contact with the notation in [25–27] let us define a shifted bases of divisors, which we denote by unhatted letters. Most of the redefinitions are trivial, namely

$$D_i = \hat{D}_i \quad \text{for } i \neq 0, \quad F_i = \hat{F}_i, \quad \text{and} \quad H_i = \hat{H}_i, \quad (3.11)$$

but the following have a deeper meaning:

$$\begin{aligned} D_0 &= \hat{F}_0 + 2\hat{H}_1 \\ D_5 &= -39\hat{D}_2 - 76\hat{D}_3 - 38\hat{D}_4 + 7\hat{F}_3 + 39\hat{F}_1 - 41\hat{F}_2 + 31\hat{F}_0 \end{aligned} \quad (3.12)$$

$D_0$  represents a physically motivated choice for our base divisor in terms of which the low-energy effective action takes a more convenient form, while  $D_5$  is the Abelian  $U(1)$ -divisor associated with the Mordell-Weil generator in the class  $[\sigma_1]$  and is obtained via the Shioda map. A convenient basis of independent divisors is given by the set

$$(D_0, D_\alpha, D_i, D_m) \equiv (D_0, H_1, D_i, D_5) . \quad (3.13)$$

Here  $D_\alpha$ ,  $\alpha = 1, \dots, h^{1,1}(\mathcal{B}_3)$  are so-called vertical divisors defined as pre-images of base divisors under the projection, i.e.  $D_\alpha = \pi^{-1}(D_\alpha^b)$ . In this particular case  $h^{1,1}(\mathbb{P}^3) = 1$  and there is only a single independent vertical divisor.

Having introduced this notation, we can compute the Green-Schwarz coefficients appearing in Eq. (2.8).  $a^\alpha$  is given by

$$c_1(\mathcal{B}_3) = a^\alpha D_\alpha^b , \quad (3.14)$$

and therefore  $a^\alpha = 2$  for our model, while  $b^\alpha$  and  $b_{(5)}^\alpha$  are the expansion coefficients of the base divisors wrapped by the GUT-divisor and the brane supporting the  $U(1)$ -factor, respectively. Here, they can be computed to be

$$b^\alpha = -\frac{D_i^2 \cdot H^2}{B \cdot H^3} = 1 \quad \text{and} \quad b_{(5)}^\alpha = -\frac{D_5^2 \cdot H^2}{B \cdot H^3} = 570 \quad (3.15)$$

and we refer to [25] for the general case.

Finally, let us comment on the fact that the appearance of a non-holomorphic zero section means that not all of the intersection numbers given in [25] hold anymore. To be precise, one only has

$$D_0 \cdot D_\Lambda \cdot D_\alpha \cdot D_\beta = 0 \tag{3.16}$$

instead of  $[D_0 \cdot D_\Lambda] = 0$  in the cohomology of all of  $X_4$ , as holds for holomorphic zero sections.

## 4 Matter and Abelian Charge Assignments

In this section we derive the matter spectrum present in the Calabi-Yau threefold and Calabi-Yau fourfold compactifications. Focusing first on the Calabi-Yau threefold we discuss the intersection theory and the split of the resolving fibers in Subsection 4.1. The  $U(1)$  charges of the fundamental matter are obtained in Subsection 4.2. We comment on the lift of these results to the Calabi-Yau fourfold. The four-dimensional chiral spectrum is then computed in Section 5.

### 4.1 Intersection Theory

By computing the discriminant of the elliptic fibration as a degree-36 polynomial over the base  $\mathbb{P}^2$  explicitly [28], one can always enumerate the codimension-two fibers where the  $I_5$  Kodaira fiber degenerates further. We now pick a sufficiently generic hypersurface using random coefficients in Eq. (3.1), find the location of the codimension-two fibers numerically, and analyze the hypersurface in these special fibers. Roughly, the hypersurface will factorize in one of the irreducible components of the toric ambient fiber, and this defines the charge of the localized matter field.

Naively, we face an impasse: the combinatorial description of the geometry of the ambient toric variety knows nothing about whether a hypersurface equation factorizes or not. Hence no toric intersection computation on the toric variety  $X_\Sigma$  can possibly capture the irreducible curves that are stuck on the codimension-two fiber; but the zero modes on those curves are precisely the matter fields that we are after. However, this argument is a bit too simple minded and, while we cannot use simply intersection theory on  $X_\Sigma$ , toric methods still apply. The trick is to construct the irreducible components of the fibers of the ambient space, which are two-dimensional toric varieties. The hypersurface restricted to the ambient toric fiber will factorize into multiple irreducible components, each of which has its own divisor class on the surface. Then all that remains is to pull back the sections to this fiber component and apply the usual toric intersection theory there.

To clarify this procedure, let us look at an example and consider the irreducible fiber component  $C_0 = \hat{D}_0 \cap \hat{H}_0$  of the  $I_5$  Kodaira fiber that intersects the zero-section  $\sigma_0$ . The star of the corresponding ray  $\langle n_{d_0} \rangle$  contains the homogeneous coordinates  $h_0$ ,

$h_1, d_1, d_2, d_4, f_0, f_1,$  and  $f_3$ . We set  $d_0$  to zero and all remaining variables to one. According to the fibration map Eq. (3.2), the point on the  $I_5$  discriminant locus  $[h_0 : h_1 : 0] \in \mathbb{P}^2$  is parametrized by the ratio of  $h_0$  and  $h_1$ , which we treat in the following as numerical constants that have been fixed to restrict us to a particular codimension-two fiber. Plugging this into the hypersurface equation, we obtain four non-zero terms

$$p(h_0, h_1, 0, d_1, d_2, 1, d_4, f_0, f_1, 1, f_3) = \beta_0 d_1 d_2^2 d_4 f_1 + \beta_1 d_1 d_2 f_0 f_1^2 + \beta_2 d_2 d_4 f_3 + \beta_3 f_0 f_1 f_3 \quad (4.1)$$

where  $\beta_0, \dots, \beta_3$  are constants depending on the fixed  $h_0, h_1$ .

For special values of the  $h_0, h_1$  the coefficients  $\beta_i$  become special and the hypersurface equation factorizes. This is how the  $I_5$  Kodaira fiber degenerates further at codimension-two fibers. A computation shows that [29]

- at 2 distinct codimension-two fibers the coefficient  $\beta_2$  vanishes and the polynomial factorizes as

$$p(h_0, h_1, 0, d_1, d_2, 1, d_4, f_0, f_1, 1, f_3) = f_1 \times (\beta_0 d_1 d_2^2 d_4 + \beta_1 d_1 d_2 f_0 f_1 + \beta_3 f_0 f_3) \quad (4.2)$$

- at 3 distinct codimension-two fibers the hypersurface equation factors as

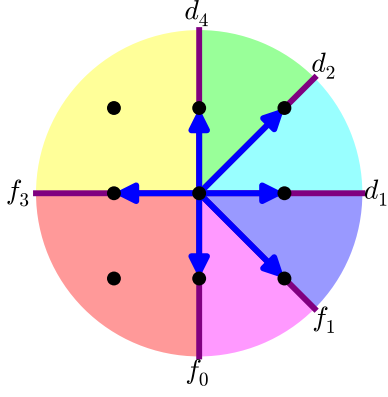
$$p(h_0, h_1, 0, d_1, d_2, 1, d_4, f_0, f_1, 1, f_3) = (\beta'_0 d_1 d_2 f_1 + \beta'_1 f_3) \times (\beta'_2 d_2 d_4 + \beta'_3 f_0 f_1) \quad (4.3)$$

- at further 14 codimension-two degenerate fibers the hypersurface equation on the fiber component  $C_0$  does not factorize. Instead, other irreducible components of the  $I_5$  fiber, that is,  $C_i = \hat{D}_i \cap \hat{H}_0$  for  $i \neq 0$ , become reducible.
- finally, there are 3 remaining codimension-two fibers where multiple  $I_5$  components factor simultaneously. This is where the **10** matter fields are localized.

To understand the intersection theory on the fiber, we have to construct the fiber component  $C_0 = \hat{D}_0 \cap \hat{H}_0$  as a toric variety. That is, the remaining homogeneous coordinates  $d_1, d_2, d_4, f_0, f_1, f_3$  on the right hand side of Eq. (4.1) are the homogeneous coordinates of a two-dimensional toric variety. The toric surface can be reconstructed from knowing how the homogeneous coordinate rescalings act. First, one has to identify the subset of homogeneous rescalings on the 4-d toric variety  $X_\Sigma$  that do not change the values of  $h_0$  and  $h_1$ . Then, ignore the action on  $d_0$  since it is being set to zero. The result is that the toric surface on which Eq. (4.1) is defined is the one shown in Figure 2. In more elaborate terms, this is the relative star construction of [30]. This toric surface is embedded into the fiber of the toric variety  $X_\sigma$  over  $[h_0 : h_1 : 0]$  via

$$i_0 : [d_1 : d_2 : d_4 : f_0 : f_1 : f_3] \mapsto [h_0 : h_1 : 0 : d_1 : d_2 : 1 : d_4 : f_0 : f_1 : 1 : f_3] \quad (4.4)$$

We now take advantage of the toric surface description of the fiber component. First, we can formulate the factorization of the hypersurface equation as follows:



Point	$n_z$	Coord. $z$	$V(z)$
1	0	$d_1$	$\bar{D}_1$
1	1	$d_2$	$\bar{D}_2$
0	1	$d_4$	$\bar{D}_4$
-1	0	$f_3$	$\bar{F}_3$
1	-1	$f_1$	$\bar{F}_1$
0	-1	$f_0$	$\bar{F}_0$

**Figure 2:** The toric ambient space fiber  $C_0$ , that is, one of the five irreducible components of  $\pi^{-1}([h_0 : h_1 : 0])$ .

- At 2 distinct codimension-two fibers, where the hypersurface factors as in Eq. (4.2), the  $I_5$  fiber component splits into two irreducible components with homology classes

$$V(p) = (\bar{F}_1) + (\bar{F}_0 + \bar{F}_3), \quad (4.5)$$

- and at 3 distinct codimension-two fibers, where the hypersurface equation factors as Eq. (4.3), the  $I_5$  fiber component splits into two irreducible components with homology classes

$$V(p) = (\bar{F}_0 + \bar{F}_1) + (\bar{F}_3). \quad (4.6)$$

Furthermore, the sections  $\sigma_0, \sigma_1$ , as divisors on  $X_\Sigma$ , can be pulled back by the embedding map  $i_0$ , see Eq. (4.4). The details of the toric algorithm for the pullback by the fiber embedding can be found in [30]. The result is that

$$\begin{aligned} i_0^*(\sigma_0) &= \bar{F}_0, \\ i_0^*(\sigma_1) &= \bar{F}_3 - \bar{F}_0. \end{aligned} \quad (4.7)$$

To summarize, the  $I_5$  Kodaira fiber degenerates at  $2 + 3$  codimension-two fibers by splitting the irreducible component intersecting the zero-section in two, yielding a fiber of Kodaira type  $I_6$ . However, in the first two fibers it splits into two curves that are distinct from the split in the last 3 fibers. The fiber components and their intersection number with the sections is given in Table 4.1.

## 4.2 Fundamental Matter

The two different degenerations of the  $I_5$  Kodaira fiber into codimension-two  $I_6$ -type fibers result in localized  $2 \times \mathbf{5}$  and  $3 \times \mathbf{5}$  matter of  $SU(5)$ . They will turn out to be distinguished by their  $U(1)$  charge, as we are about to see. The  $U(1)$  charge is given by the intersection of the curves stuck at codimension-two fiber, that is, the irreducible

$I_6$ component	$\bar{C}_0$	$\bar{C}_1$	$\bar{C}_2$	$\bar{C}_3$	$\bar{C}_4$	$\bar{C}_5$
Realization	$F_0 + F_1$	$F_3$	$C_1$	$C_2$	$C_3$	$C_4$
$\cap \sigma_0$	0	1	0	0	0	0
$\cap \sigma_1$	1	-1	0	0	1	0

$I_6$ component	$\bar{C}_0$	$\bar{C}_1$	$\bar{C}_2$	$\bar{C}_3$	$\bar{C}_4$	$\bar{C}_5$
Realization	$F_3$	$F_0 + F_1$	$C_1$	$C_2$	$C_3$	$C_4$
$\cap \sigma_0$	1	0	0	0	0	0
$\cap \sigma_1$	-1	1	0	0	1	0

**Table 4.1:** Intersection numbers of the two different  $I_6$ -type codimension-two fibers where the codimension-one  $I_5$  fiber splits the fiber component intersecting the zero section. The curves  $\bar{C}_i$  are the  $I_6$  fiber components in cyclic order. The curves  $C_i$  are the  $I_5$  fiber components  $C_i = \hat{D}_i \cap \hat{H}_0$ .

components of the factored  $I_5$  component, with the image of the section under the Shioda map [15]  $S : MW(X) \rightarrow H_4(X, \mathbb{Q})$ . For a single  $I_5$  Kodaira fiber, this boils down to

$$\begin{aligned}
U(1)\text{-charge}(\bar{C}_i) &= \bar{C}_i \cap S(\sigma_1) \\
&= \bar{C}_i \cap \sigma_1 - \bar{C}_i \cap \sigma_0 + \sum_{1 \leq a, b \leq 4} (\bar{C}_i \cap \hat{D}_a) \begin{pmatrix} 4 & 3 & 2 & 1 \\ \hline \sigma_1 & \sigma_1 & \sigma_1 & \sigma_1 \\ \sigma_1 & \sigma_1 & \sigma_1 & \sigma_1 \\ \sigma_1 & \sigma_1 & \sigma_1 & \sigma_1 \\ \sigma_1 & \sigma_1 & \sigma_1 & \sigma_1 \end{pmatrix}_{ab} (\sigma_1 \cap C_b) \quad (4.8)
\end{aligned}$$

For example, consider  $\bar{C}_0 = \bar{F}_0 + \bar{F}_1$ , a curve contributing to the  $2 \times \mathbf{5}$ . Its intersections with  $\sigma_0, \sigma_1$  are listed in the upper half of Table 4.1.

$$U(1) - \text{charge}(2 \times \mathbf{5}) = 1 - 0 + (0 \ 0 \ 0 \ 1) \begin{pmatrix} 4 & 3 & 2 & 1 \\ \hline \sigma_1 & \sigma_1 & \sigma_1 & \sigma_1 \\ \sigma_1 & \sigma_1 & \sigma_1 & \sigma_1 \\ \sigma_1 & \sigma_1 & \sigma_1 & \sigma_1 \\ \sigma_1 & \sigma_1 & \sigma_1 & \sigma_1 \end{pmatrix} \begin{pmatrix} 0 \\ 0 \\ 1 \\ 0 \end{pmatrix} = \frac{8}{5} \quad (4.9)$$

Similarly, the  $U(1)$  charge of the other  $3 \times \mathbf{5}$  ends up being  $\frac{7}{5}$ . As noted in Subsection 4.1, there are further 14 codimension-two fibers giving rise to  $\mathbf{5}$  and 3 more yielding  $\mathbf{10}$  matter. Their  $U(1)$  charge can be computed by straightforward application of the same methods and we will leave the details as an exercise to the reader. The result is that, after clearing denominators to make the  $U(1)$  charges integral, the  $SU(5)$ -charged spectrum is

$$2 \times \mathbf{5}_8 + 3 \times \mathbf{5}_7 + 6 \times \mathbf{5}_3 + 8 \times \mathbf{5}_2 + 3 \times \mathbf{10}_1. \quad (4.10)$$

The Calabi-Yau fourfold will have the same types of representations arising, since they are determined by the behaviour at a generic point on a matter curve. In other words, after intersecting the matter curve with a divisor crossing it, the same analysis for the  $SU(5) \times U(1)$  representation content applies. Of course, the 6-d quaternionic representations will be split up into conjugate pairs of 4-d representations, and the multiplicity of the representations will be different. In fact, the multiplicities do depend on the four-form flux which is a phenomenon for fourfolds that has no threefold analogue, and will be the topic of the following section.

## 5 Chiral Index from One-Loop Chern-Simons Terms

In this final section we compute the four-dimensional chiral indexes for the matter spectrum induced by an F-theory compactification on the Calabi-Yau fourfold of Subsection 3.3. We first make some general remarks on  $G_4$  fluxes and their induced three-dimensional Chern-Simons terms in Subsection 5.1. The explicit computations of the chiral indices for our example are presented in Subsection 5.2.

### 5.1 General Remarks on $G_4$ -Fluxes and Chiralities

Naively reducing the six-dimensional matter multiplets to four dimensions, the resulting matter representations appear in vector-like pairs. Thus, the resulting theory is non-chiral. However, this changes as soon as fourform fluxes are included on the M-theory side. Effectively, their inclusion is equivalent to projecting out certain matter multiplets, hence leading to non-trivial chiral indices. The complete data of an F-theory compactification to four dimensions therefore consists of the Calabi-Yau fourfold  $X_4$  supplemented by a choice of G-flux satisfying certain consistency conditions. We will now explain what these conditions are, construct a concrete set of fluxes and calculate the resulting chiral indices.

First of all, a consistent choice of  $G_4$  must satisfy a quantisation condition [31], i.e.

$$G_4 + \frac{1}{2}c_2(\hat{X}_4) \in H^4(\hat{X}_4, \mathbb{Z}) , \quad (5.1)$$

where  $c_2(\hat{X}_4)$  is the second Chern class of  $\hat{X}_4$ . Furthermore, the fourth cohomology group of  $\hat{X}_4$  splits into orthogonal subspaces, namely a horizontal one whose elements are derived from complex structure variations of the global  $(4,0)$ -form on  $\hat{X}_4$  and a vertical one. The vertical subspace contains four-forms obtained by taking the wedge product of two  $(1,1)$ -forms on  $\hat{X}_4$ . While horizontal fluxes give rise to a non-trivial flux superpotential, the vertical fluxes induce chirality in the four-dimensional theory and we therefore concentrate on them. For more details on flux quantisation in F-theory, we refer to [32,33]. Chirality induced by G-fluxes has recently been studied in [1–3, 10, 25, 34–38]. We will follow the general approach of [25, 37].

In order to determine the chiral indices a given flux induces, we employ a result obtained by using M-/F-theory duality in three and four dimensions, respectively. On the M-theory side, non-trivial G-flux induces a Chern-Simons term in three dimensions

$$S_{CS}^{(3)} = -\frac{1}{2} \int \Theta_{AB}^M A^A \wedge F^B , \quad (5.2)$$

with flux coefficients

$$\Theta_{AB}^M = \frac{1}{2} \int_{X_4} G_4 \wedge \omega_A \wedge \omega_B . \quad (5.3)$$

and  $\omega_A$  the basis of  $(1,1)$ -forms introduced in Subsection 3.3. On the F-theory side, Chern-Simons terms originate from integrating out charged matter in the circle reduction



from four to three dimensions and one can show that their coefficients are given by

$$\Theta_{\Lambda\Sigma}^F = - \sum_{\mathbf{R}} \chi(\mathbf{R}) \sum_{\mathbf{w} \in \mathbf{R}} \mathbf{w}_\Lambda \mathbf{w}_\Sigma \text{sign}(\mathbf{w}) \quad (5.4)$$

Here  $\Lambda, \Sigma = (i, 5)$ ,  $\mathbf{R}$  runs over all complex representations and  $\mathbf{w}$  are the weights of a representation  $\mathbf{R}$ . To each weight  $\mathbf{w}$  one can naturally assign a curve in  $X_4$  and we take  $\text{sign}(\mathbf{w})$  to be +1 if this curves shrinks to a point in the F-theory limit  $X_4 \rightarrow \hat{X}_4$  and  $-1$  otherwise. For details of how to calculate  $\text{sign}(\mathbf{w})$  we refer to [25, 37], where analogous computations were carried out.

Before giving an explicit form of  $G_4$ , we impose some additional constraints:

$$\begin{aligned} \Theta_{i\alpha} = \Theta_{\alpha\beta} = \Theta_{0\alpha} = 0 \\ \Theta_{0i} = \Theta_{00} = 0 \end{aligned} \quad (5.5)$$

The first three equations forbid a broken non-Abelian gauge group, non-geometric fluxes and fluxes along the 3d/4d-circle respectively. For holomorphic zero sections the remaining two constraints follow automatically from the first three and therefore we impose them by hand for our rational zero section.

After enforcing the constraints in Eq. (5.5), the only other non-vanishing Chern-Simons terms apart from (5.4) are  $\Theta_{05}$ . A loop calculation on the F-Theory side determines them to be [25]

$$\Theta_{05}^F = \frac{1}{6} \sum_q n(q)q, \quad (5.6)$$

where  $n(q)$  counts the number of fields with  $U(1)$  charge  $q$ . For example, in the case of our spectrum one has that

$$n(-1) - n(+1) = 10\chi(\mathbf{10}_{-1}) \quad (5.7)$$

since every  $\mathbf{10}$  representation has ten different weights. Note that the matching condition  $\Theta_{05}^F = \Theta_{05}^M$  is precisely equivalent to the cancellation of the gravitational-abelian anomaly in Eq. (2.8), since  $\Theta_{05} = \frac{1}{2}\Theta_{\alpha 5}$ .

## 5.2 Chiral Matter Spectrum in the Example

For the triangulation (A.2) we find four independent flux parameters, namely

$$\begin{aligned}
G_4 = & \alpha \left( 2D_2^2 - 28D_3D_4 - 7D_4^2 + \frac{9}{4}F_3^2 - \frac{28}{5}D_2F_1 + 4F_1^2 + \frac{11}{10}F_3F_2 + \frac{122}{15}F_1F_2 - \frac{36}{5}F_2^2 \right. \\
& \left. - \frac{65}{6}F_1F_0 - 9F_0^2 \right) + \beta \left( -D_2^2 + 8D_3D_4 + 2D_4^2 - \frac{1}{2}F_3^2 + \frac{6}{5}D_2F_1 - \frac{1}{5}F_3F_2 - \frac{49}{15}F_1F_2 \right. \\
& \left. + \frac{12}{5}F_2^2 + 3F_1F_0 + 2F_0^2 \right) + \gamma \left( -D_2^2 + 8D_3D_4 + 2D_4^2 - \frac{1}{2}F_3^2 + \frac{6}{5}D_2F_1 + \frac{11}{5}F_3F_2 \right. \\
& \left. - \frac{47}{15}F_1F_2 + \frac{8}{5}F_2^2 + 3F_1F_0 + 2F_0^2 \right) + \delta \left( -2D_2^2 + 20D_3D_4 + 5D_4^2 - \frac{7}{4}F_3^2 + \frac{12}{5}D_2F_1 \right. \\
& \left. + \frac{11}{10}F_3F_2 - \frac{118}{15}F_1F_2 + \frac{24}{5}F_2^2 + \frac{21}{2}F_1F_0 + 7F_0^2 \right).
\end{aligned} \tag{5.8}$$

Given  $G_4$ , one can match the flux-induced Chern-Simons coefficients with those produced by chiral matter on the F-theory side by solving

$$\Theta_{\Lambda\Sigma}^M = \Theta_{\Lambda\Sigma}^F. \tag{5.9}$$

There is a small ambiguity in solving (5.9) for the chiral indices, since the two  $SU(5)$ -singlets give proportional contributions. We therefore demand that the theory is anomaly-free and obtain the unique solution

$$\begin{aligned}
\chi(\mathbf{5}_{-8}) &= \alpha, & \chi(\mathbf{5}_{-3}) &= \beta, & \chi(\mathbf{5}_2) &= \gamma, & \chi(\mathbf{5}_7) &= \delta, \\
\chi(\mathbf{10}_{-1}) &= -\alpha - \beta - \gamma - \delta, & \chi(\mathbf{1}_5) &= -8\alpha + \beta + 4\gamma + 11\delta, \\
\chi(\mathbf{1}_{10}) &= -5\alpha + 8\gamma + 14\delta.
\end{aligned} \tag{5.10}$$

Let us stress that it is a non-trivial consistency check that all four anomaly conditions in Eq. (2.8) are satisfied, since the above ambiguity only gave us one free parameter.

Last of all, we remark that the Euler number  $\chi(X_4)$  and

$$\frac{1}{2} \int_{X_4} G_4 \wedge G_4 \tag{5.11}$$

can easily be calculated using the same toric methods for any choice of flux parameters. We checked that the tadpole condition can be easily satisfied by constraining the flux parameters. Our particular fourfold has  $\chi(X_4) = 2364$ .

## Acknowledgements

We like to thank Eran Palti, Raffaele Savelli, and Timo Weigand. The work of T.G. and J.K. was supported by a research grant of the Max Planck Society. V.B. was supported by the Dublin Institute for Advanced Studies. V.B. would also like to thank Pas de la Casa for a pleasant surrounding while this work was being finished.

# A Details on the Calabi-Yau Geometries

## A.1 Toric Construction

In the main text we listed the rays of the fan defining the threefold in Table 3.1, and for the fourfold in Eq. (3.9). To uniquely determine the ambient toric variety (and, therefore, the Calabi-Yau hypersurface) it is necessary to also list the generating cones of the fan. Different choices for the fan will result in different intersection numbers, but not in different  $U(1)$  charges. For the threefold hypersurface, we pick

$$\begin{aligned} \Sigma = \{ & \langle \hat{H}_0 \hat{F}_0 \hat{H}_1 \hat{F}_1 \rangle, \langle \hat{H}_0 \hat{F}_2 \hat{H}_1 \hat{F}_1 \rangle, \langle \hat{D}_0 \hat{H}_0 \hat{F}_3 \hat{F}_0 \rangle, \langle \hat{D}_0 \hat{F}_3 \hat{F}_0 \hat{H}_1 \rangle, \langle \hat{H}_0 \hat{F}_3 \hat{F}_0 \hat{H}_1 \rangle, \\ & \langle \hat{H}_0 \hat{F}_3 \hat{F}_2 \hat{D}_3 \rangle, \langle \hat{F}_3 \hat{F}_2 \hat{D}_3 \hat{H}_1 \rangle, \langle \hat{H}_0 \hat{F}_3 \hat{F}_2 \hat{H}_1 \rangle, \langle \hat{H}_0 \hat{D}_1 \hat{D}_2 \hat{F}_1 \rangle, \langle \hat{H}_0 \hat{F}_2 \hat{D}_2 \hat{F}_1 \rangle, \\ & \langle \hat{H}_0 \hat{F}_2 \hat{D}_3 \hat{D}_2 \rangle, \langle \hat{D}_1 \hat{H}_1 \hat{D}_2 \hat{F}_1 \rangle, \langle \hat{F}_2 \hat{H}_1 \hat{D}_2 \hat{F}_1 \rangle, \langle \hat{F}_2 \hat{D}_3 \hat{H}_1 \hat{D}_2 \rangle, \langle \hat{D}_0 \hat{H}_0 \hat{D}_1 \hat{F}_1 \rangle, \\ & \langle \hat{D}_0 \hat{H}_0 \hat{F}_0 \hat{F}_1 \rangle, \langle \hat{D}_0 \hat{H}_0 \hat{D}_1 \hat{D}_2 \rangle, \langle \hat{D}_0 \hat{F}_0 \hat{H}_1 \hat{F}_1 \rangle, \langle \hat{D}_0 \hat{D}_1 \hat{H}_1 \hat{F}_1 \rangle, \langle \hat{D}_0 \hat{D}_1 \hat{H}_1 \hat{D}_2 \rangle, \\ & \langle \hat{H}_0 \hat{F}_3 \hat{D}_3 \hat{D}_4 \rangle, \langle \hat{D}_0 \hat{H}_0 \hat{F}_3 \hat{D}_4 \rangle, \langle \hat{D}_0 \hat{F}_3 \hat{H}_1 \hat{D}_4 \rangle, \langle \hat{F}_3 \hat{D}_3 \hat{H}_1 \hat{D}_4 \rangle, \langle \hat{D}_0 \hat{H}_0 \hat{D}_2 \hat{D}_4 \rangle, \\ & \langle \hat{H}_0 \hat{D}_3 \hat{D}_2 \hat{D}_4 \rangle, \langle \hat{D}_3 \hat{H}_1 \hat{D}_2 \hat{D}_4 \rangle, \langle \hat{D}_0 \hat{H}_1 \hat{D}_2 \hat{D}_4 \rangle \} \end{aligned} \quad (\text{A.1})$$

and for the fourfold hypersurface we are using

$$\begin{aligned} \Sigma = \{ & \langle \hat{H}_0 \hat{H}_1 \hat{H}_2 \hat{F}_3 \hat{F}_2 \rangle, \langle \hat{H}_0 \hat{H}_1 \hat{H}_2 \hat{F}_3 \hat{F}_0 \rangle, \langle \hat{H}_0 \hat{H}_1 \hat{H}_2 \hat{F}_1 \hat{F}_2 \rangle, \langle \hat{H}_0 \hat{H}_1 \hat{H}_2 \hat{F}_1 \hat{F}_0 \rangle, \\ & \langle \hat{H}_0 \hat{H}_1 \hat{D}_0 \hat{D}_1 \hat{D}_2 \rangle, \langle \hat{H}_0 \hat{H}_1 \hat{D}_0 \hat{D}_1 \hat{F}_1 \rangle, \langle \hat{H}_0 \hat{H}_1 \hat{D}_0 \hat{D}_2 \hat{D}_4 \rangle, \langle \hat{H}_0 \hat{H}_1 \hat{D}_0 \hat{D}_4 \hat{F}_3 \rangle, \\ & \langle \hat{H}_0 \hat{H}_1 \hat{D}_0 \hat{F}_3 \hat{F}_0 \rangle, \langle \hat{H}_0 \hat{H}_1 \hat{D}_0 \hat{F}_1 \hat{F}_0 \rangle, \langle \hat{H}_0 \hat{H}_1 \hat{D}_1 \hat{D}_2 \hat{F}_1 \rangle, \langle \hat{H}_0 \hat{H}_1 \hat{D}_2 \hat{D}_3 \hat{D}_4 \rangle, \\ & \langle \hat{H}_0 \hat{H}_1 \hat{D}_2 \hat{D}_3 \hat{F}_2 \rangle, \langle \hat{H}_0 \hat{H}_1 \hat{D}_2 \hat{F}_1 \hat{F}_2 \rangle, \langle \hat{H}_0 \hat{H}_1 \hat{D}_3 \hat{D}_4 \hat{F}_3 \rangle, \langle \hat{H}_0 \hat{H}_1 \hat{D}_3 \hat{F}_3 \hat{F}_2 \rangle, \\ & \langle \hat{H}_0 \hat{H}_2 \hat{D}_0 \hat{D}_1 \hat{D}_2 \rangle, \langle \hat{H}_0 \hat{H}_2 \hat{D}_0 \hat{D}_1 \hat{F}_1 \rangle, \langle \hat{H}_0 \hat{H}_2 \hat{D}_0 \hat{D}_2 \hat{D}_4 \rangle, \langle \hat{H}_0 \hat{H}_2 \hat{D}_0 \hat{D}_4 \hat{F}_3 \rangle, \\ & \langle \hat{H}_0 \hat{H}_2 \hat{D}_0 \hat{F}_3 \hat{F}_0 \rangle, \langle \hat{H}_0 \hat{H}_2 \hat{D}_0 \hat{F}_1 \hat{F}_0 \rangle, \langle \hat{H}_0 \hat{H}_2 \hat{D}_1 \hat{D}_2 \hat{F}_1 \rangle, \langle \hat{H}_0 \hat{H}_2 \hat{D}_2 \hat{D}_3 \hat{D}_4 \rangle, \\ & \langle \hat{H}_0 \hat{H}_2 \hat{D}_2 \hat{D}_3 \hat{F}_2 \rangle, \langle \hat{H}_0 \hat{H}_2 \hat{D}_2 \hat{F}_1 \hat{F}_2 \rangle, \langle \hat{H}_0 \hat{H}_2 \hat{D}_3 \hat{D}_4 \hat{F}_3 \rangle, \langle \hat{H}_0 \hat{H}_2 \hat{D}_3 \hat{F}_3 \hat{F}_2 \rangle, \\ & \langle \hat{H}_1 \hat{H}_2 \hat{D}_0 \hat{D}_1 \hat{D}_2 \rangle, \langle \hat{H}_1 \hat{H}_2 \hat{D}_0 \hat{D}_1 \hat{F}_1 \rangle, \langle \hat{H}_1 \hat{H}_2 \hat{D}_0 \hat{D}_2 \hat{D}_4 \rangle, \langle \hat{H}_1 \hat{H}_2 \hat{D}_0 \hat{D}_4 \hat{F}_3 \rangle, \\ & \langle \hat{H}_1 \hat{H}_2 \hat{D}_0 \hat{F}_3 \hat{F}_0 \rangle, \langle \hat{H}_1 \hat{H}_2 \hat{D}_0 \hat{F}_1 \hat{F}_0 \rangle, \langle \hat{H}_1 \hat{H}_2 \hat{D}_1 \hat{D}_2 \hat{F}_1 \rangle, \langle \hat{H}_1 \hat{H}_2 \hat{D}_2 \hat{D}_3 \hat{D}_4 \rangle, \\ & \langle \hat{H}_1 \hat{H}_2 \hat{D}_2 \hat{D}_3 \hat{F}_2 \rangle, \langle \hat{H}_1 \hat{H}_2 \hat{D}_2 \hat{F}_1 \hat{F}_2 \rangle, \langle \hat{H}_1 \hat{H}_2 \hat{D}_3 \hat{D}_4 \hat{F}_3 \rangle, \langle \hat{H}_1 \hat{H}_2 \hat{D}_3 \hat{F}_3 \hat{F}_2 \rangle \} . \end{aligned} \quad (\text{A.2})$$

We note that these fans have been constructed such that they are compatible with the projection that we want to use as a toric morphism.

## A.2 Showing the Existence of a Section

In this appendix we show that the homology class (3.8) actually contain a section, or does not only happen to have the right intersection numbers with fiber components. To settle this question we have to compute the line bundle cohomology group  $H_0(X, \mathcal{O}_X(s))$ . This cohomology group sits in the long exact sequence for the sheaf exact sequence

$$0 \longrightarrow \mathcal{O}_{X_\Sigma}(s + K_{X_\Sigma}) \longrightarrow \mathcal{O}_{X_\Sigma}(s) \longrightarrow \mathcal{O}_X(s) \longrightarrow 0 \quad (\text{A.3})$$

for the restriction from the four-dimensional ambient toric variety to the three-dimensional Calabi-Yau hypersurface. The toric cohomology groups can easily be computed to be

$$\dim H^i(X_\Sigma, \mathcal{O}_{X_\Sigma}(s + K_{X_\Sigma})) = \begin{cases} 1 & i = 1, \\ 0 & \text{else,} \end{cases} \quad \dim H^i(X_\Sigma, \mathcal{O}_{X_\Sigma}(s)) = 0. \quad (\text{A.4})$$

Therefore, the long exact sequence

$$\begin{aligned} \cdots \longrightarrow H^0(X_\Sigma, \mathcal{O}_{X_\Sigma}(s)) \longrightarrow H^0(X, \mathcal{O}_X(s)) \longrightarrow \\ \longrightarrow H^1(X_\Sigma, \mathcal{O}_{X_\Sigma}(s + K_{X_\Sigma})) \longrightarrow H^1(X_\Sigma, \mathcal{O}_{X_\Sigma}(s)) \longrightarrow \cdots \end{aligned} \quad (\text{A.5})$$

tells us that the homology class  $[\sigma_1] = [\hat{F}_1 - \hat{F}_0 - \hat{D}_0 - \hat{D}_3 - \hat{D}_4 + \hat{H}_0]$  contains a unique variety  $\sigma_1$  representing it.

## References

- [1] Ron Donagi and Martijn Wijnholt. Model Building with F-Theory. *Adv.Theor.Math.Phys.*, 15:1237–1318, 2011.
- [2] Chris Beasley, Jonathan J. Heckman, and Cumrun Vafa. GUTs and Exceptional Branes in F-theory - I. *JHEP*, 0901:058, 2009.
- [3] Chris Beasley, Jonathan J. Heckman, and Cumrun Vafa. GUTs and Exceptional Branes in F-theory - II: Experimental Predictions. *JHEP*, 0901:059, 2009.
- [4] Timo Weigand. Lectures on F-theory compactifications and model building. *Class.Quant.Grav.*, 27:214004, 2010.
- [5] Anshuman Maharana and Eran Palti. Models of Particle Physics from Type IIB String Theory and F-theory: A Review. 2012.
- [6] Ralph Blumenhagen, Thomas W. Grimm, Benjamin Jurke, and Timo Weigand. Global F-theory GUTs. *Nucl.Phys.*, B829:325–369, 2010.
- [7] Thomas W. Grimm, Sven Krause, and Timo Weigand. F-Theory GUT Vacua on Compact Calabi-Yau Fourfolds. *JHEP*, 1007:037, 2010.

- [8] Ching-Ming Chen, Johanna Knapp, Maximilian Kreuzer, and Christoph Mayrhofer. Global  $SO(10)$  F-theory GUTs. *JHEP*, 1010:057, 2010.
- [9] Johanna Knapp, Maximilian Kreuzer, Christoph Mayrhofer, and Nils-Ole Walliser. Toric Construction of Global F-Theory GUTs. *JHEP*, 1103:138, 2011.
- [10] Joseph Marsano and Sakura Schafer-Nameki. Yukawas, G-flux, and Spectral Covers from Resolved Calabi-Yau's. *JHEP*, 1111:098, 2011.
- [11] David R. Morrison and Cumrun Vafa. Compactifications of F theory on Calabi-Yau threefolds. 2. *Nucl.Phys.*, B476:437–469, 1996.
- [12] Paul S. Aspinwall and David R. Morrison. Nonsimply connected gauge groups and rational points on elliptic curves. *JHEP*, 9807:012, 1998.
- [13] Paul S. Aspinwall, Sheldon H. Katz, and David R. Morrison. Lie groups, Calabi-Yau threefolds, and F theory. *Adv.Theor.Math.Phys.*, 4:95–126, 2000.
- [14] Thomas W. Grimm and Timo Weigand. On Abelian Gauge Symmetries and Proton Decay in Global F-theory GUTs. *Phys.Rev.*, D82:086009, 2010.
- [15] David R. Morrison and Daniel S. Park. F-Theory and the Mordell-Weil Group of Elliptically-Fibered Calabi-Yau Threefolds. *JHEP*, 1210:128, 2012.
- [16] Christoph Mayrhofer, Eran Palti, and Timo Weigand.  $U(1)$  symmetries in F-theory GUTs with multiple sections. 2012.
- [17] Joseph Marsano, Natalia Saulina, and Sakura Schafer-Nameki. Monodromies, Fluxes, and Compact Three-Generation F-theory GUTs. *JHEP*, 0908:046, 2009.
- [18] Joseph Marsano, Natalia Saulina, and Sakura Schafer-Nameki. Compact F-theory GUTs with  $U(1)$  (PQ). *JHEP*, 1004:095, 2010.
- [19] Emilian Dudas and Eran Palti. On hypercharge flux and exotics in F-theory GUTs. *JHEP*, 1009:013, 2010.
- [20] Eran Palti. A Note on Hypercharge Flux, Anomalies, and  $U(1)$ s in F-theory GUTs. 2012.
- [21] Antonella Grassi and David R. Morrison. Group representations and the Euler characteristic of elliptically fibered Calabi-Yau threefolds. 2000.
- [22] Volker Braun, Thomas W. Grimm, and Jan Keitel. Systematics of Global F-theory GUTs with  $U(1)$  symmetries.
- [23] R. Wazir. Arithmetic on Elliptic Threefolds. *ArXiv Mathematics e-prints*, December 2001.

- [24] Antonella Grassi and Vittorio Perduca. Weierstrass models of elliptic toric K3 hypersurfaces and symplectic cuts. 2012.
- [25] Mirjam Cvetič, Thomas W. Grimm, and Denis Klevers. Anomaly Cancellation And Abelian Gauge Symmetries In F-theory. 2012.
- [26] Thomas W. Grimm and Raffaele Savelli. Gravitational Instantons and Fluxes from M/F-theory on Calabi-Yau fourfolds. *Phys.Rev.*, D85:026003, 2012.
- [27] Thomas W. Grimm. The N=1 effective action of F-theory compactifications. *Nucl.Phys.*, B845:48–92, 2011.
- [28] Volker Braun. Toric Elliptic Fibrations and F-Theory Compactifications. *JHEP*, 1301:016, 2013.
- [29] David R. Morrison and Washington Taylor. Matter and singularities. 2011.
- [30] Y. Hu, C.-H. Liu, and S.-T. Yau. Toric morphisms and fibrations of toric Calabi-Yau hypersurfaces. *ArXiv Mathematics e-prints*, October 2000.
- [31] Edward Witten. On flux quantization in M theory and the effective action. *J.Geom.Phys.*, 22:1–13, 1997.
- [32] Andres Collinucci and Raffaele Savelli. On Flux Quantization in F-Theory. *JHEP*, 1202:015, 2012.
- [33] Andres Collinucci and Raffaele Savelli. On Flux Quantization in F-Theory II: Unitary and Symplectic Gauge Groups. *JHEP*, 1208:094, 2012.
- [34] Hirotaka Hayashi, Radu Tatar, Yukinobu Toda, Taizan Watari, and Masahito Yamazaki. New Aspects of Heterotic–F Theory Duality. *Nucl.Phys.*, B806:224–299, 2009.
- [35] Andreas P. Braun, Andres Collinucci, and Roberto Valandro. G-flux in F-theory and algebraic cycles. *Nucl.Phys.*, B856:129–179, 2012.
- [36] Sven Krause, Christoph Mayrhofer, and Timo Weigand.  $G_4$  flux, chiral matter and singularity resolution in F-theory compactifications. *Nucl.Phys.*, B858:1–47, 2012.
- [37] Thomas W. Grimm and Hirotaka Hayashi. F-theory fluxes, Chirality and Chern-Simons theories. *JHEP*, 1203:027, 2012.
- [38] Moritz Kuntzler and Sakura Schafer-Nameki. G-flux and Spectral Divisors. *JHEP*, 1211:025, 2012.